©Operative Dentistry, 2014, **39-2,** E57-E70

Measurement of the Internal Adaptation of Resin Composites Using Micro-CT and Its Correlation With Polymerization Shrinkage

HJ Kim • SH Park

Clinical Relevance

Resin composites with low levels of polymerization shrinkage strain and stress resulted in better internal adaptation. This effect may be related to the low incidence of complications, such as postoperative hypersensitivity.

SUMMARY

In the present study, the internal adaptation of dentin-composite interfaces with various resin composite materials under conditions of thermomechanical loading was analyzed nondestructively using micro–computed tomography (micro-CT), and these results were compared with analyses of microgaps after sectioning. Additionally, the correlation of internal adaptation with polymerization shrinkage strain and stress was evaluated.

Four nonflowable resins, Gradia Direct (GD), Filtek P90 (P9), Filtek Z350 (Z3), and Charisma (CH), and two flowable resins, SDR (SD) and Tetric N-Flow (TF) were used. First, the polymerization shrinkage strain and stress were measured. Then, Class I cavities were prepared in 48 premolars. They were divided randomly into six groups, and the cavities were filled with composites using XP bond. To evaluate the internal adaptation, tooth specimens were immersed in a 25% silver nitrate solution, and micro-CT analysis was performed before and after thermomechanical loading. The silver nitrate penetration (%SP) was measured. After buccolingual sectioning and rhodamine penetration of the specimen, the rhodamine penetration (%RP) was measured using a stereomicroscope. One-way analysis of variance was then used to compare the polymerization shrinkage strain, stress, %SP, and %RP among the groups at a 95% confidence level. A paired *t*-test was used to compare the %SP before and after thermomechanical loading. Pearson correlation analysis was used to compare the correlation between polymerization shrinkage strain/stress and %SP or %RP to a 95% confidence level.

Evaluation of the polymerization shrinkage strain demonstrated that P9 < Z3 ≤ GD < CH

Hyun-Joo Kim, MS, Yonsei University, Conservative Dentistry, Oral Science Research Center, Seoul, Republic of Korea

*Sung-ho Park, PhD, Yonsei University, Conservative Dentistry, Oral Science Research Center, Seoul, Republic of Korea

*Corresponding author: 134, Shinchon-dong, Seodaemun-gu, Seoul, 120-752, Republic of Korea; e-mail: sunghopark@yuhs.ac

DOI: 10.2341/12-378-L

≤ SD < TF ($p<0.05$); similarly, evaluation of the polymerization shrinkage stress showed that P9 ≤ GD ≤ Z3 ≤ CH ≤ SD < TF ($p<0.05$). The %SP showed that P9 ≤ GD ≤ Z3 < CH ≤ SD < TF ($p<0.05$) before loading and that P9 ≤ GD ≤ Z3 ≤ CH ≤ SD < TF ($p<0.05$) after loading. There was a significant difference between the before-loading and after-loading measurements in all groups ($p<0.05$). Additionally, there was a positive correlation between the %SP and the %RP ($r=0.810$, $p<0.001$).

Conclusively, the polymerization shrinkage stress and strain were found to be closely related to the internal adaptation of the resin composite restorations. The newly proposed model for the evaluation of internal adaptation using micro-CT and silver nitrate may provide a new measurement for evaluating the internal adaptation of restorations in a nondestructive way.

INTRODUCTION

Resin composites are generally used as restorative materials because of their good esthetics and ability to adhere to tooth structure using adhesive. However, the conversion of the resin composite monomers into a polymer network is accompanied by a bulk contraction leading to 1.67%-5.68% volumetric polymerization shrinkage.[1] Polymerization shrinkage generates stress at the tooth-restoration interface and may lead to microgap formation and microleakage, the latter of which allows for the infiltration of saliva and bacteria. This infiltration can lead to secondary caries, pathologic pulpal changes, and restoration failures.[2]

Souza-Junior and others[3] evaluated the internal adaptation of restorations by sectioning the samples. In their study, internal gaps formed prominently at the pulpal and axio-pulpal line angles of the restorations. The gap formation could cause fluid flow in the dentin tubules, and the transduction of dentinal fluid through the dentin adhesive could produce dentinal fluid-filled regions, which could contribute to the degeneration of adhesives.[4] The internal adaptation of dentin-restoration interfaces has generally been evaluated by dye penetration with basic fuchsin, methylene blue, erythrosin, silver nitrate, or radioactive markers and by sectioning the samples.[5] Although very popular, the dye penetration method exhibits inherent limitations in that the type, size, and concentration of the tracer, the pH of the aqueous immersion solutions, and the chemical affinity of the tracer with hard dental tissues all influence the results obtained.[6] Furthermore, sectioning destroys the sample and renders additional testing impossible, and gaps measured in a selective area cannot represent the entire sample.[7]

For these reasons, direct imaging techniques with micro–computed tomography (micro-CT) are becoming more widely used.[8] Micro-CT obtains the three-dimensional (3D) structures of small objects with a high level of spatial resolution. In dental research, micro-CT imaging has been used to analyze the structures at dentin-adhesive-composite interfaces before and after mechanical loading[9] and to evaluate resin composite volume and 3D marginal adaptation before and after polymerization.[6,10] However, such studies did not use dentin adhesives, and their clinical relevance was therefore very low. Kwon and Park[11] evaluated the internal adaptation of adhesive restorations with and without a resin-modified glass ionomer base using micro-CT analysis of human molars. Using micro-CT and the silver nitrate infiltration technique through the dentinal tubules of the pulpal side, the dentin-composite resin interface was evaluated nondestructively.

It is challenging to develop restorative materials that do not produce microgaps, and the current research on new materials is insufficient. To evaluate restorative materials, further research about internal adaptation and microleakage will therefore be very important.

The aim of this study was to evaluate the internal adaptation of resin composites using the nondestructive technique of micro-CT, to compare these results with the microgaps found in histologic sections, and to evaluate their correlation with polymerization shrinkage.

The null hypotheses are as follows.

1) No differences exist in the internal adaptation among the resin composites tested with micro-CT.

2) No correlation exists between polymerization shrinkage stress/strain and internal adaptation tested with micro-CT.

3)No correlation exists between the internal adaptation tested with micro-CT and the microgaps evaluated with microscopy and the dye solution.

4) No correlation exists between the polymerization shrinkage stress/strain and the microgaps evaluated with microscopy and the dye solution.

METHODS AND MATERIALS

This study was approved by the local ethics committee (IRB 2-2012-0060).

Table 1: *Composite Materials Used in This Study*[a]

Code	Product	Manufacturer	Base Resin	Filler, wt%/vol%	EM, GPa
P9	Filtek P90	3M ESPE, St Paul, MN, USA	Silorane-based	76%/55%	9.6
GD	Gradia Direct	GC Co, Milford, DE, USA	UDMA dimethacrylate co-monomers	73%/64%	6.3
Z3	Filtek Z350	3M ESPE, St Paul, MN, USA	Bis-GMA/EMA, UDMA	78.5%/59.5%	11
CH	Charisma	Heraeus Kulzer, Dormagen, Germany	Bis-GMA, TEGDMA	78%/61%	8
SD	SDR	Dentsply Caulk, Milford, DE, USA	Modified urethane dimethacrylate EBPADMA/TEGDMA	68%/45%	5.7
TF	Tetric N-flow	Ivoclar Vivadent, Schaan, Liechtenstein	Bis-GMA, TEGDMA	63.8%/43%	5.3

Abbreviations: P9, Filtek P90; GD, Gradia Direct; Z3,Filtek Z350; CH, Charisma; SD, SureFil SDR; TF, Tetric N- flow; Bis-GMA, bisphenol A dimethacrylate; Bis-EMA, bisphenol A polyethylene glycol diether dimethacrylate; EBPADMA, ethoxylated bisphenol A dimethacrylate; EM, elastic modulus; TEGDMA: triethyleneglycol dimethacrylate; UDMA, urethane dimethacrylate.

[a] *Base resin composition, filler content and elastic modulus are from manufacturer's technical reports and information.*

Materials

Six different resin composite materials were used. These resin composite materials and their compositions are listed in Table 1.

Polymerization Shrinkage Strain Measurements

Resin composites were transferred to a circular Teflon mold (diameter 4.5 mm, depth 1.3 mm) to ensure that the same volume of resin composite was used for each linometer sample. Next, the materials were transferred to an aluminum disk in a custom-made linometer (R&B Inc, Daejon, Korea) that had previously been coated with a separating glycerin gel, covered with a glass slide, and loaded under constant pressure (Figure 1). The specimens were then light-cured with an LED-type light-curing unit (800 mW/cm^2, Bluephase, Ivoclar Vivadent, Schaan,

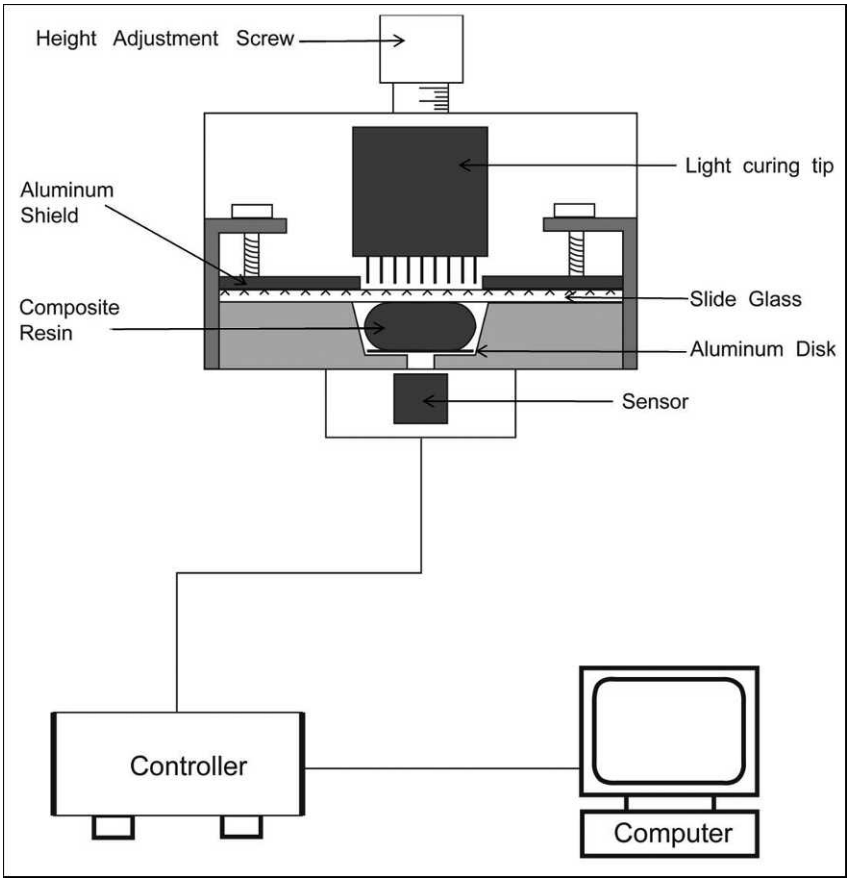

Figure 1. *A schematic diagram of the custom-made linometer.*

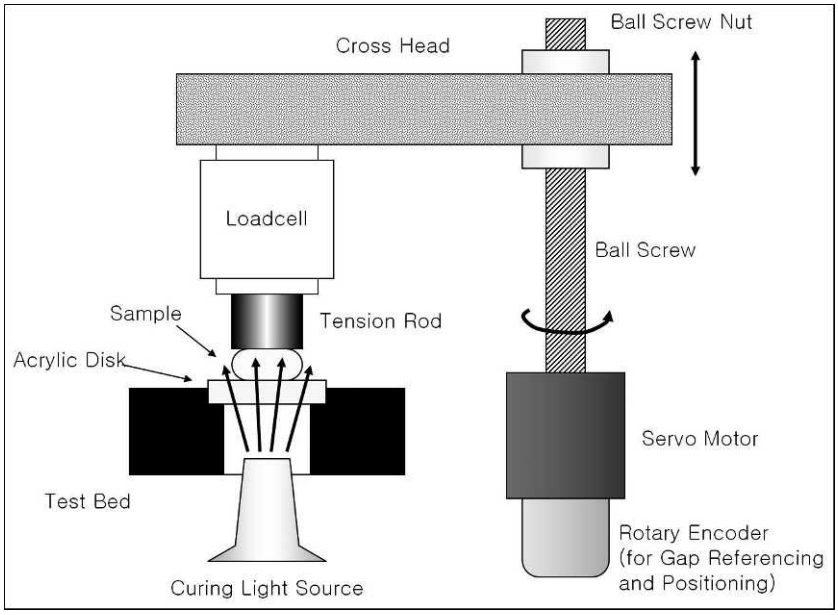

Figure 2. *A schematic drawing of the custom-made polymerization shrinkage stress-measuring machine with a sample in place.*

Liechtenstein) for 40 seconds. The tip of the curing light was positioned 2 mm above the glass slide to ensure the proper curing of the specimens. As the resin composite under the slide glass was cured, it moved the aluminum disk under the resin composite upward. The amount of disk displacement, which was caused by the linear shrinkage of the resin composite, was measured using an eddy current sensor every 0.5 seconds for a period of 120 seconds (Figure 1).

Polymerization Shrinkage Stress Measurements

Polymerization shrinkage stress was measured with a custom-made device and software (R&B Inc) (Figure 2). Resin composite (0.3 g) was transferred to an acrylic disc, and the upper tension rod was set to ensure that the thickness of the specimen was 1 mm (Figure 2). The stress status between the tension rod and the resin composite was set to zero using the software before light curing. Then, the specimens were light-cured with an LED-type light-curing unit (800 mW/cm^2, Bluephase, Ivoclar Vivadent) for 40 seconds through the acrylic disc (Figure 2). At this time, the polymerization shrinkage stress developed, and they were measured by a load cell connected to the tension rod and computer (Figure 2). The software program recorded the polymerization shrinkage stress data simultaneously in the computer every 0.5 seconds for a period of 180 seconds.

Internal Adaptation Measurements

Specimens—Forty-eight intact human premolars extracted for orthodontic treatment were used. In the selecting process, each tooth's dimensions were measured, and the size deviations were controlled within 1 mm. In addition, the thickness of hard tissue, the size of pulp spaces, and the position of pulp horns were evaluated using digital x-ray, and attempts were made to standardize them as far as possible. A high-speed coarse diamond bur (959 KR 314.018, tapered cylinder style with round corner, grit size 100 μm, Komet GEBR Brasseler GmbH & Co KG, Lemgo, Germany) was used to amputate the roots from the cervical regions of the premolars and to prepare occlusal cavities (4 mm mesiodistally, 6 mm buccolingually, 4-mm depth at central portion). The bur was replaced after every eight teeth. Using digital radiographs and the associated software, the distance between the cavity floors and the pulp chambers was controlled to be within 1.0 mm. The 48 specimens were divided randomly into six groups.

The interior parts of the cavities were etched with 10% phosphoric acid (ALL-ETCH, Bisco Inc, Schaumburg IL, USA) for 15 seconds. After irrigation with water for 15 seconds, the cavities were gently dried with an air syringe. For all groups, the dentin adhesive (XP bond, Dentsply Caulk, Milford, DE, USA) was applied for 20 seconds and then air-dried for 5 seconds according to the manufacturer's recommendations. Then, it was cured for 20 seconds

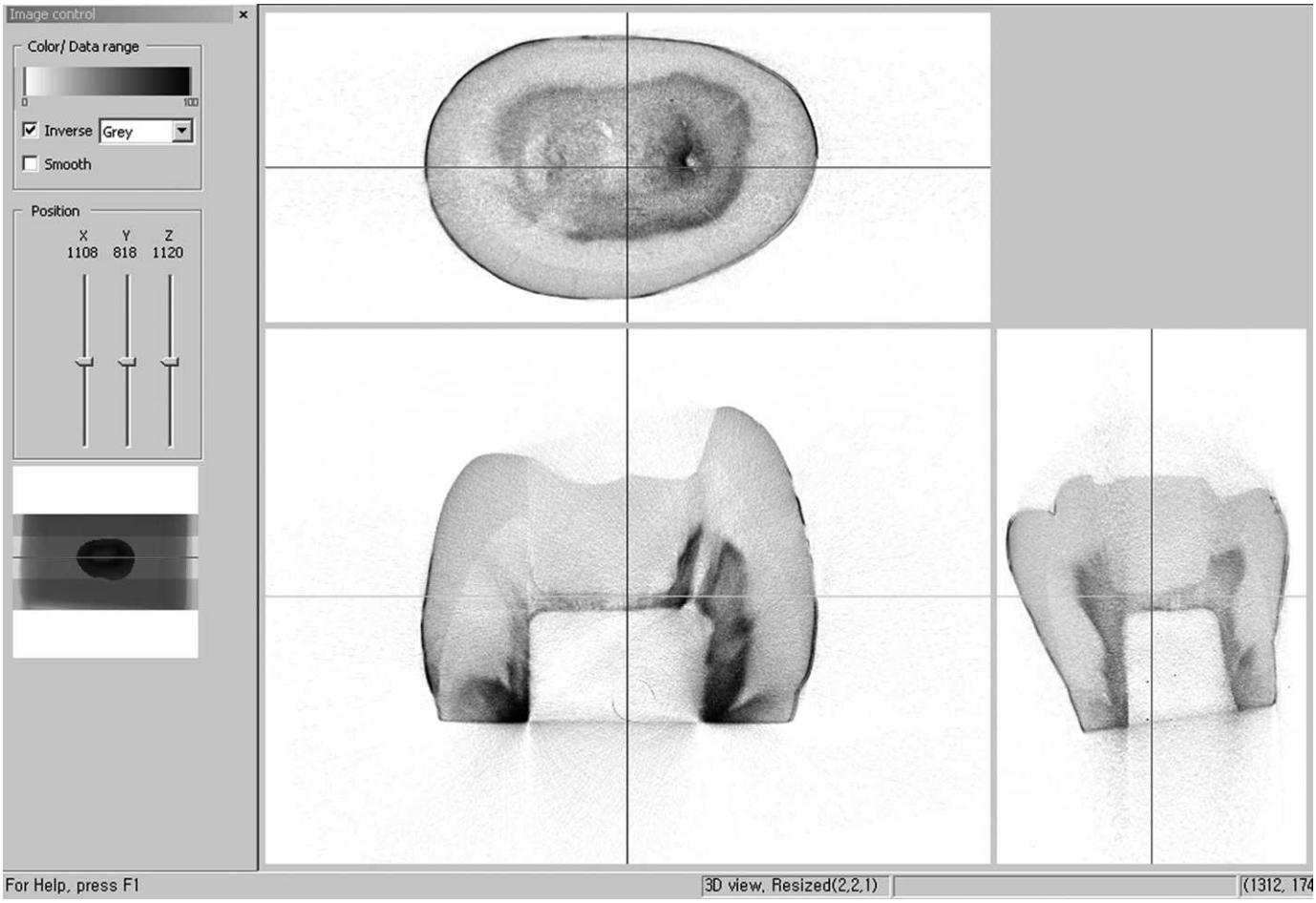

Figure 3. *Reconstruction of the coronal view using the DataViewer program.*

using an LED-type light-curing unit (800 mW/cm^2, Bluephase, Ivoclar Vivadent). The density power of the curing lights was measured using an integration sphere and its software (Gigahertz-Optic GmbH, Puchheim, Germany). For all groups except SDR, the resin composites were applied in two 2-mm increments. For each increment, the resin composites were cured with the LED-type light-curing unit for 20 seconds. SDR was applied as 4 mm of bulk filling and was then cured with the LED-type light-curing unit for 20 seconds, according to the manufacturer's instructions.

Silver Nitrate Solution Application—The pulp chambers were soaked in 17% ethylenediamine tetraacetic acid for 5 minutes and were then washed with saline. The teeth were immersed in a 25% silver nitrate solution under a pressure of 3 kgf for three days.

Thermomechanical Loading With a Chewing Simulator—A chewing simulator CS-4.8 (SD Mechatronik, Feldkirchen-Westerham, Germany) was used to apply a mechanical load of 5 kgf (49 N) 600,000 times under thermodynamic conditions (5°-55°C, dwell time 60 seconds, transfer time 24 seconds). The chewing simulator has eight chambers that simulate vertical and horizontal movements simultaneously under thermodynamic conditions. Each of the chambers consists of an upper sample holder that can fasten the specimen with a screw and a lower plastic sample holder in which the specimen can be embedded.

Micro-CT and Image Analysis—A high-resolution micro-CT (Model 1076, SkyScan, Aartselaar, Belgium) was used to take micrographs under conditions of 100 kV accelerating voltage, a 100 μA beam current, a 0.5 mm Al filter, 18 μm resolution, and 360° rotation at the 0.5° step. Two-dimensional images of 550-560 sagittal and coronal views of each specimen were taken two times (preloading and postloading). During this procedure, each tooth specimen was mounted in a special template that

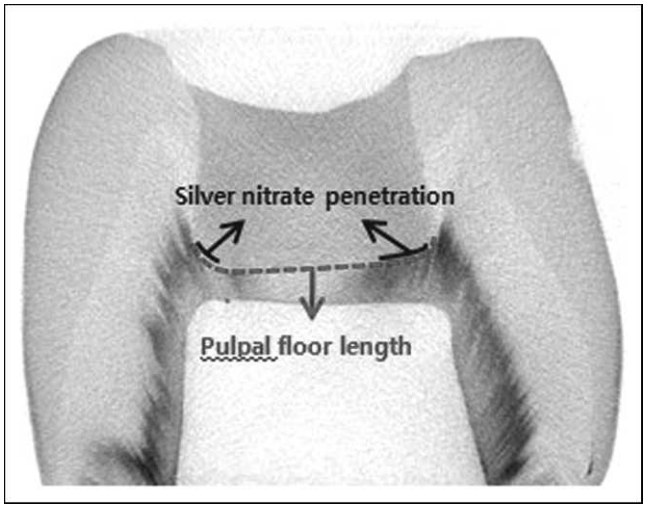

Figure 4. *The %SP calculation method: (silver nitrate penetration length/pulpal wall length) × 100.*

was made specifically for that specimen. This template minimized the change in specimen position during repeated micro-CT imaging. The 2D images were analyzed using the CTAn (SkyScan) and DataViewer (SkyScan) programs. Before image analysis, the density of tooth structure and restoration was measured using the DataViewer (SkyScan) program (dentin: 40-65; resin composite: 90-130; silver nitrate 125-180). The silver penetration into the microgap between the tooth and the restorative materials was considered to be valid when the densities were over the 141 index, which was based on the observation that the areas that were clearly penetrated by the silver nitrate solution had densities >141 on the index when the sagittal and coronal images were compared for the same phase (Figure 3).

Among the 2D images of each specimen, 100 images were selected that clearly confirmed the relationship between the pulpal floors and the silver nitrate. For each specimen, a selection of 2D images was collected before and after mechanical loading; this collection was produced by selecting 100 cuts of 2D images arranged at equal intervals beginning from the central regions of the mesiodistal distances of cavities. The length of the margin of the pulpal floor with a microgap or intact margin was calculated for each image of each specimen, and all the data were then collected and summed. The ratio of the silver nitrate penetration length into the microgap between the tooth and the restoration to the length of the pulpal floor was calculated for each specimen (%SP) (Figure 4). The %SP was calculated as (silver nitrate penetration length/pulpal floor length) × 100.

Table 2: *Amount of Linear Shrinkage and Shrinkage Rate (SD), n=10**

Code	Average, μm	Strain Rate, μm/sec
P9	3.42 (0.91)[a]	0.43 (0.04)[a]
GD	13.40 (1.25)[b]	1.24 (0.15)[b]
Z3	10.98 (1.03)[b]	1.09 (0.19)[b]
CH	23.38 (1.39)[c]	1.87 (0.08)[c]
SD	25.40 (1.82)[c]	2.15 (0.14)[d]
TF	35.48 (3.42)[d]	2.88 (0.22)[e]

Abbreviations: P9, Filtek P90; GD, Gradia Direct; Z3,Filtek Z350; CH, Charisma; SD, SureFil SDR; TF, Tetric N- flow
** Different letters indicate different linear shrinkage values at p<0.05 level.*

Stereomicroscope Evaluation After Sectioning—To validate the results obtained from the micro-CT, teeth were prepared for stereomicroscope analysis. After the specimens were embedded in an acrylic resin, they were sectioned buccolingually using a low-speed diamond saw (500 rpm, Isomet, Buehler, IL, USA) and then polished with 1200-grit SiC paper. After embedding the samples in a 1% rhodamine solution for 24 hours, the resulting microgaps were evaluated using a stereomicroscope (Leica S8APO, Leica Microsystems, Wetzlar, Germany) at 120x magnification. The ratio of the rhodamine and silver nitrate penetration length into the microgap to the full pulpal floor length, was calculated for each specimen (%RP). The %RP was calculated as (rhodamine penetration + silver nitrate penetration length/pulpal floor length) × 100.

Statistical Analysis

One-way analysis of variance (ANOVA) was used to compare the polymerization shrinkage strain and stress among the groups. Scheffe analysis was used for post hoc analysis. Additionally, polymerization shrinkage strain and stress rate was calculated at 10 seconds of light curing, and then they were compared using the same statistical method.

One-way ANOVA was used to compare the %SP among the groups before and after loading. A paired *t*-test was used to compare the %SP before and after thermomechanical loading. Scheffe analysis was used for post hoc analysis. All statistical inferences made were within a 95% confidence interval.

Pearson correlation analysis was used to compare the correlation between polymerization shrinkage strain/stress and %SP or %RP. The correlation between %SP after thermomechanical loading and %RP was also evaluated.

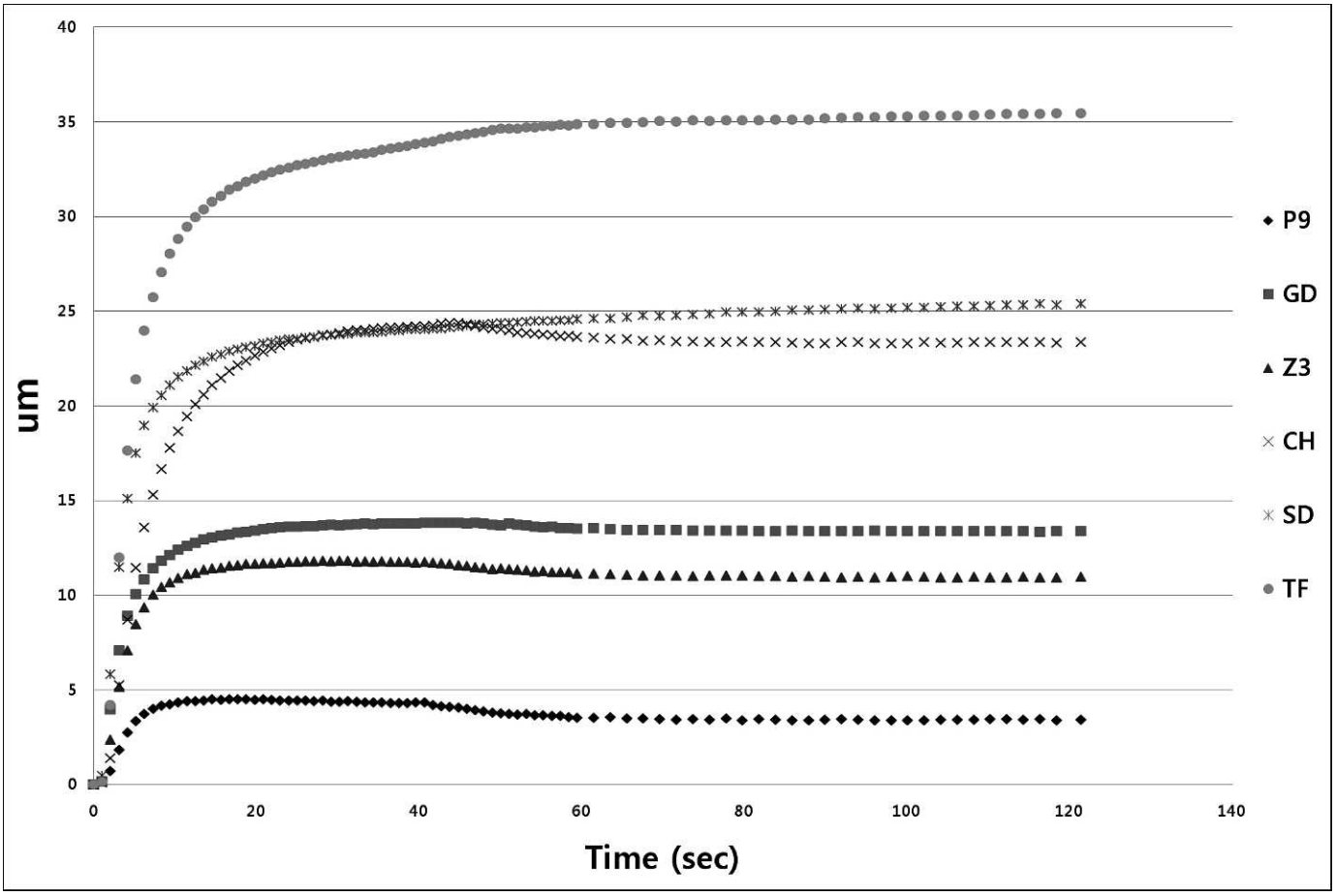

Figure 5. *The change of the linear polymerization shrinkage vs time.*

RESULTS

Polymerization Shrinkage Strain

The amount of polymerization shrinkage strain and strain rate are summarized in Table 2. The amount of polymerization shrinkage strain from least to greatest was P9 < Z3 ≤ GD < CH ≤ SD < TF ($p<0.05$). The shrinkage strain rate was P9 < Z3 ≤ GD < CH < SD < TF ($p<0.05$). The pattern of polymerization shrinkage strain for the materials is shown in Figure 5.

Table 3: *Amount of Shrinkage Stress and Stress Rate (SD), n=8**

Code	Stress, kgf	Stress rate, kgf
P9	1.78 (0.45)[a]	0.11 (0.04)[a]
GD	2.28 (0.24)[ab]	0.13 (0.02)[ab]
Z3	2.48 (0.15)[bc]	0.14 (0.02)[bc]
CH	2.87 (0.31)[bc]	0.15 (0.01)[bc]
SD	3.07 (0.15)[c]	0.17 (0.01)[c]
TF	4.01 (0.37)[d]	0.22 (0.02)[d]

Abbreviations: P9, Filtek P90; GD, Gradia Direct; Z3,Filtek Z350; CH, Charisma; SD, SureFil SDR; TF, Tetric N- flow
** Different letters indicate different shrinkage stress values at p<0.05 level.*

Polymerization Shrinkage Stress

The amount and rate of polymerization shrinkage stress are summarized in Table 3. The amount and rate of polymerization shrinkage stress from least to greatest was P9 < Z3 ≤ GD < CH ≤ SD < TF ($p<0.05$). The pattern of polymerization shrinkage stress for the studied materials is shown in Figure 6.

General Aspects of Silver Nitrate Penetration

In the nonflowable resin group (GD, P9, Z3, and CH), the silver nitrate solution was distributed uniformly throughout the entire pulpal floor region, and a few air bubbles were observed inside the composite resin. The amount of silver nitrate penetration increased after mechanical loading; this change in the penetra-

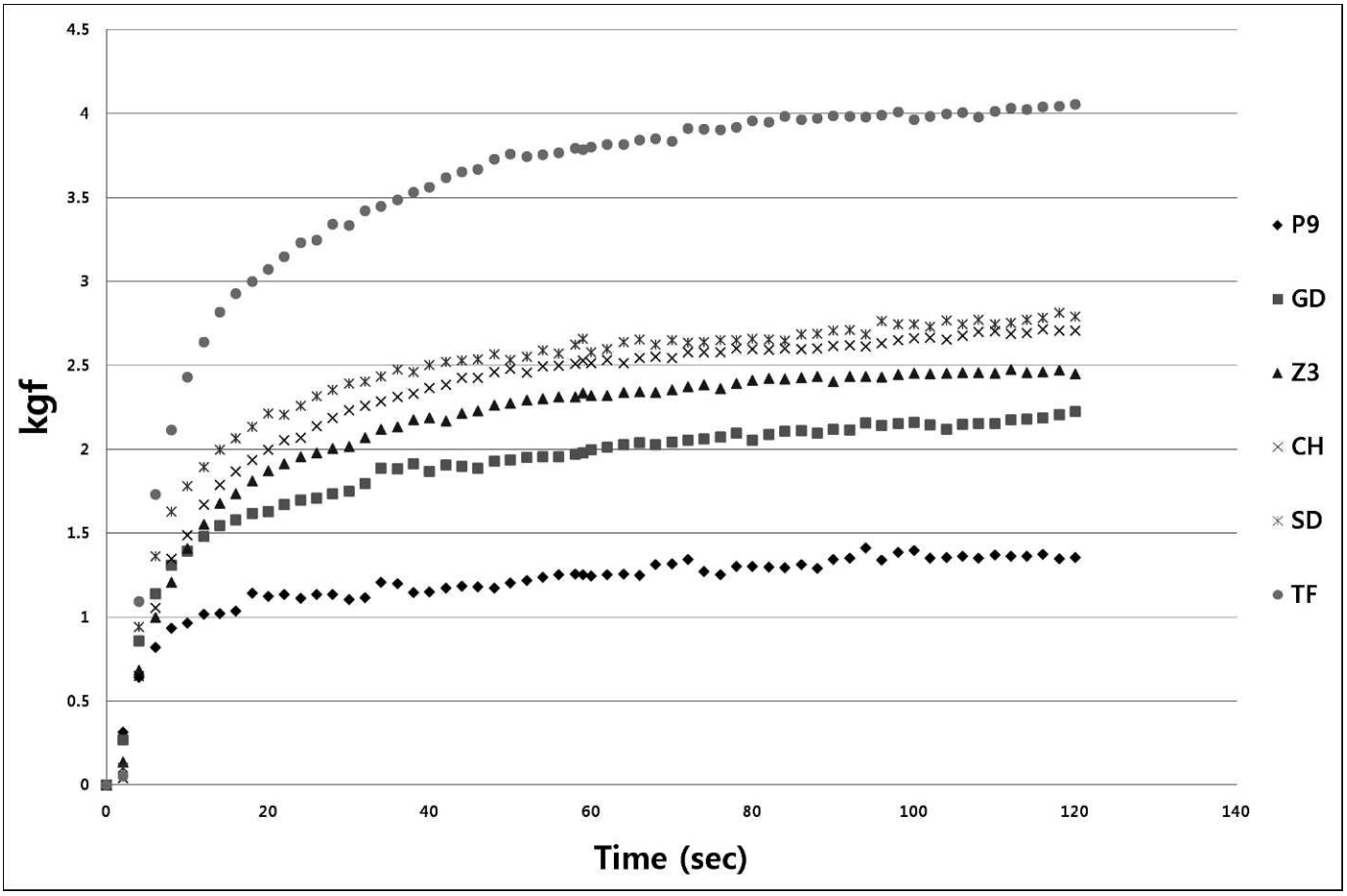

Figure 6. *The change of the polymerization stress vs time.*

tion quantities appeared to be the largest in the Z3 group.

In the flowable resin group (SD and TF), few air bubbles or defects were observed within resin composite material. The silver nitrate solution primarily penetrated the axio-pulpal line angle regions compared with the nonflowable resin. Before mechanical loading, a large amount of silver nitrate penetrated the specimens (Figure 7). However, the change in the penetration quantities after mechanical loading was smaller than in the nonflowable group.

%SP Evaluation

Table 4 and Figure 8 list the mean %SP and the associated standard deviations. The materials were ranked by %SP in the order P9 $\leq$ GD $\leq$ Z3 $<$ CH $\leq$ SD $<$ TF ($p<0.05$) before mechanical loading and P9 $\leq$ GD $\leq$ Z3 $\leq$ CH $\leq$ SD $<$ TF ($p<0.05$) after mechanical loading. In all groups, there was a significant difference between the values before and after mechanical loading ($p<0.05$).

%RP

The materials were ranked by %RP in the order P9 $\leq$ GD $\leq$ Z3 $\leq$ CH $\leq$ SD $\leq$ TF ($p<0.05$) (Table 5). The %RP had higher values and standard deviations than the %SP. The thickness of adhesive agent was between 60 and 90 μm in the middle area of the cavity floor and between 80 and 110 μm in the cavity corners.

Correlation Analysis

There was a positive correlation between the polymerization shrinkage strain/stress and %SP or %RP ($p<0.001$) (Table 6). They all showed medium to high correlations. There was a positive correlation between the %SP and %RP evaluation models ($p<0.001$, Pearson correlation constant 0.810).

DISCUSSION

The polymerization shrinkage of resin composite materials generates stress at the tooth-restoration

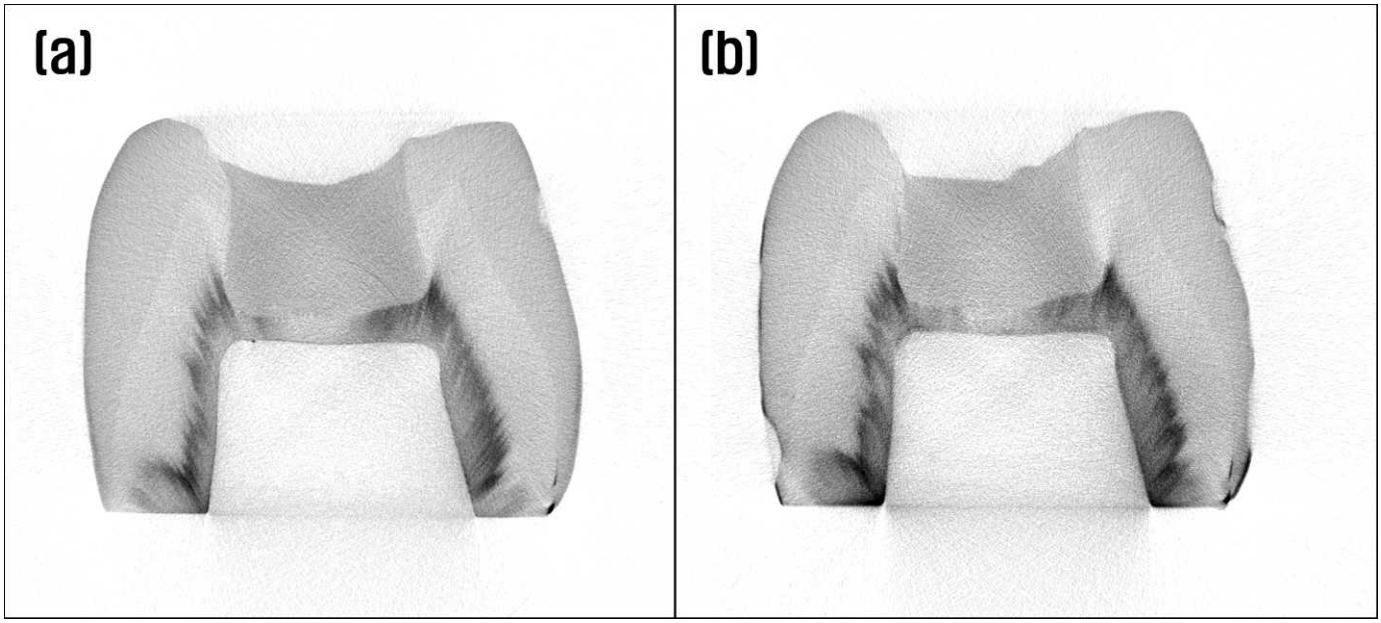

Figure 7. *Silver nitrate penetration. (a): Before mechanical loading. (b): After mechanical loading.*

interface and may clinically lead to the formation of marginal gaps. Several studies have been performed addressing the clinical relevance of this phenomenon with respect to *in vitro* microleakage. The correlation between polymerization shrinkage strain and microleakage[12-14] and the correlation between polymerization shrinkage stress and microleakage[15,16] have been evaluated. However, these studies have generally evaluated the microleakage of the marginal gap rather than the internal adaptation. To evaluate the correlation between the polymerization shrinkage strain/stress results and the internal adaptation generated by tooth stress in the present study, silver nitrate infiltration and micro-CT analysis were used. The factors influencing the stress formation included the volumetric polymerization shrinkage, the elastic modulus, the configuration factor of the restoration, the curing method used, and the adherence of the resin composite to the cavity walls.[17] In the present study, the cavity size and type, the curing mode, and the dentin adhesive were uniform across all specimens; only the resin composite material was varied.

Table 4: *Mean Percent and SD of Silver Nitrate Penetrate Length to Whole Pulpal Wall Length (%SP)†*

Thermomechanical Loading

Code	Before		After	
	Average	SD	Average	SD
P9	17.6[a]	2.4	24.4[a]	3.3*
GD	20.6[a]	2.8	26.8[a]	2.9*
Z3	21.9[a]	4.9	29.5[ab]	5.4*
CH	28.0[b]	4.4	34.7[bc]	3.4*
SD	33.8[b]	5.9	38.0[c]	6.3*
TF	46.0[c]	10.0	49.8[d]	10.1*

Abbreviations: P9, Filtek P90; GD, Gradia Direct; Z3,Filtek Z350; CH, Charisma; SD, SureFil SDR; TF, Tetric N- flow
† Eight teeth were used for each group and 100 images were used for each tooth for %SP analysis. Different letters indicate different penetration % level among filling materials ($p<0.05$) before and after thermomechanical loading, respectively.
** Significant differences in penetration %between before and after thermomechanical loading ($p<0.05$).*

The micro-CT data collection and the silver nitrate penetration length measurements were performed according to previous study protocols.[11] Because a restorative material with a radio-density similar to that of dentin might show background noise,[18] sagittal and coronal images of the same phase were compared with the DataViewer (Sky-Scan) program. The materials were ranked by %SP in the order P9 $\leq$ GD $\leq$ Z3 $<$ CH $\leq$ SD $<$ TF ($p<0.05$) before thermomechanical loading and P9 $\leq$ GD $\leq$ Z3 $\leq$ CH $\leq$ SD $<$ TF ($p<0.05$) after the loading. Before thermomechanical loading, %SP might show the internal adaptation of the initial condition. P9 had a lower %SP and TF had a higher %SP than the other groups. All of the nonflowable resins (P9, GD, and Z3) except CH had a lower %SP than the flowable resins (SD, TF) ($p<0.05$). After thermocycling loading, the ranks of the materials were similar to those before thermomechanical loading. It implies that the initial internal adapta-

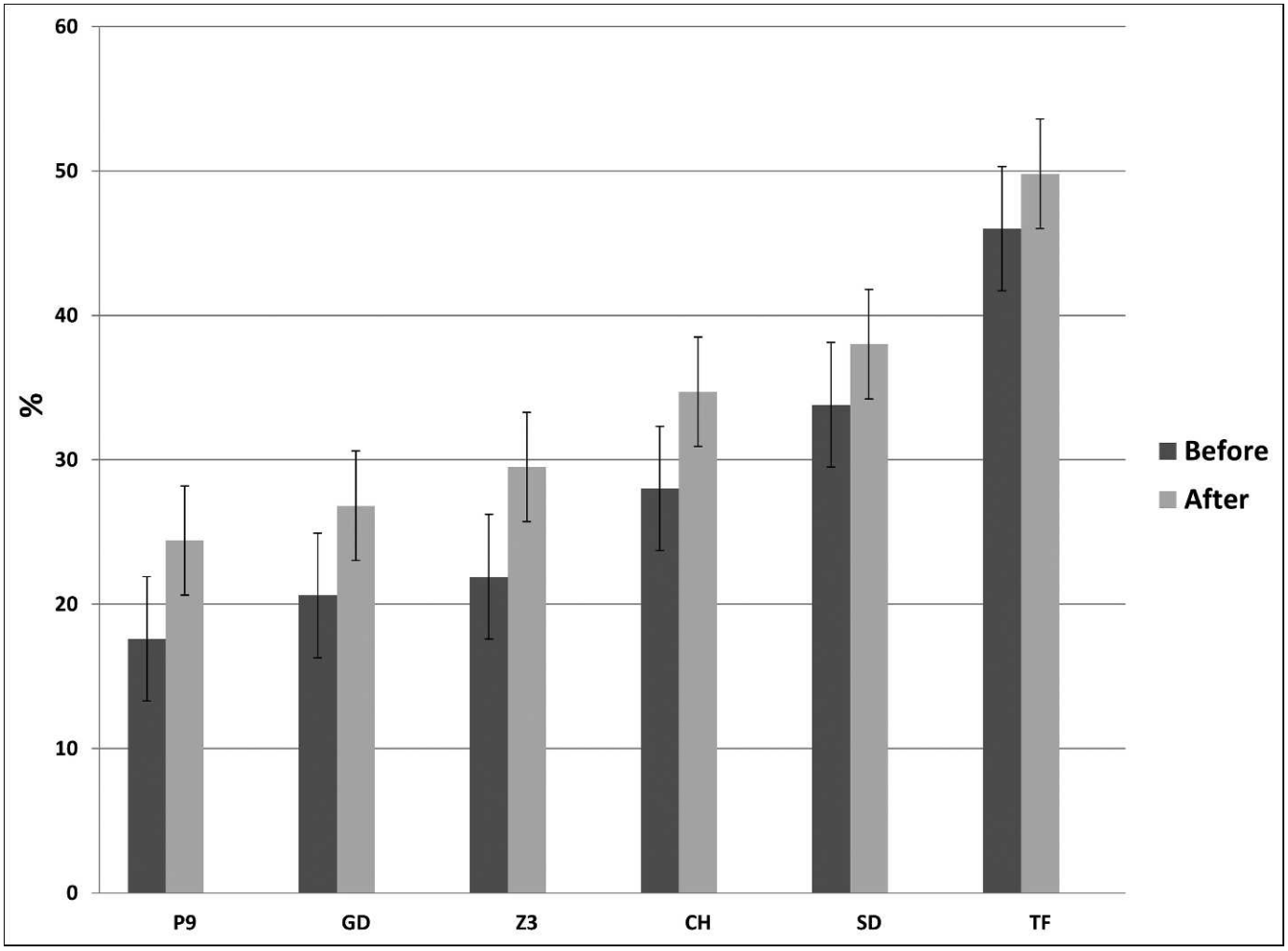

Figure 8. *Mean percent (%) and standard deviation of the silver nitrate penetration length relative to the pulpal wall length before and after thermomechanical loading.*

tion may affect the adaptation after thermomechanical loading. Considering the high correlation between %SP and polymerization shrinkage stress and strain (Table 6), the higher %SP values in flowable composites seems to be related with higher shrinkage strain/strain values than nonflowable composites.

Table 5: *Mean Percent and SD of Total Rhodamine Penetrate Length to Whole Pulpal Wall Length (%RP)) (n=8 for Each Group)**

Code	Total Microgap	SD
P9	34.4[a]	10.8
GD	36.7[a]	9.2
Z3	37.1[a]	9.1
CH	41.7[ab]	11.8
SD	49.1[ab]	11.9
TF	55.3[ab]	10.9

Abbreviations: P9, Filtek P90; GD, Gradia Direct; Z3,Filtek Z350; CH, Charisma; SD, SureFil SDR; TF, Tetric N- flow
** Different letters indicate different microgap values at $p<0.05$ level.*

In the present study, a chewing simulator was used to simulate clinical situations. In all groups, there was a significant difference before and after thermomechanical loading, and it was consistent with the results of a previous study.[11] The difference in %SP before and after mechanical loading was 3%-4% in the flowable resin groups (SD and TF) and 6%-8% in the nonflowable composite groups (GD, P9, Z3, and CH). This difference might be due to the stress-absorbing ability of the flowable resin, which has a low elastic modulus, making it possible to minimize the destruction of the adhesion of the restoration.[19] After thermomechanical loading, the correlation between the polymerization shrinkage strain and stress and the %SP was reduced (Table 6). Mechan-

Table 6: *Pearson Correlation Constant*[a]

Thermomechanical Loading	%SP		%RP
	Before	After	After
Polymerization shrinkage strain	0.805	0.777	0.655
Polymerization shrinkage stress	0.819	0.785	0.686

Abbreviations: P9, Filtek P90; GD, Gradia Direct; Z3,Filtek Z350; CH, Charisma; SD, SureFil SDR; TF, Tetric N- flow
[a] *%SP is equal to (silver nitrate penetration length/pulpal floor length)×100. %RP is calculated as (rhodamine penetration + silver nitrate penetration length/pulpal floor length)×100.*

ical properties such as the elastic modulus might affect the results in this period.

In the flowable resin groups, silver nitrate penetration was concentrated in the axio-pulpal line angle regions. These results are similar to those obtained from a photoelastic model that measured the stress distribution of teeth with resin composite restorations.[20] Another possible cause might be a difference in the application method. Whereas hand instruments were used to pack the composites into the cavities in the nonflowable composites, the flowable resins were injected into them, and packing was therefore not necessary.[21]

To validate the results obtained from the micro-CT, all specimens were sectioned and evaluated by stereomicroscope. There was a high correlation between the %RP and the %SP ($p<0.001$, Pearson correlation constant 0.810). This observation shows that the micro-CT and silver nitrate penetration techniques can be used alternatively for the evaluation of internal adaptation. In certain cases in which silver nitrate had previously penetrated the gap, it was very difficult to detect the rhodamine penetration because the intense black shade of the silver nitrate could prevent the detection of the red rhodamine shade. In these cases, the silver nitrate penetration length was added to the rhodamine penetration length for the %RP calculations because the microgap was evident.

In all cases, the %RP had a higher value than the %SP. This result might be due to the destructive nature of the sectioning process. This may also show the limitations of the dye penetration and sectioning methods. The correlation between the %RP and the polymerization shrinkage strain and stress was lower than that of the %SP (Table 6). It is assumed that the destructive sectioning procedure affected the %RP.

The factors that influence polymerization shrinkage include monomer molecular weight and concentration and filler size and concentration.[22] GD, P9, Z3, and CH all have higher filler content than the flowable composites, SD and TF. These high-filler resin composites have a lower monomer content that participates in the polymerization process, which is related to the lower polymerization shrinkage. Although the space occupied by the filler particles does not participate in the curing contraction, high filler loads may require low-molecular-weight monomers to ensure a proper handling viscosity. In low-viscosity materials, the motility of the monomers is active, such that a higher proportion of monomers participates in the polymerization process, increasing the polymerization shrinkage.[23] In the present study, CH exhibits significantly higher levels of polymerization shrinkage strain than the other nonflowable resins tested because of its high TEGDMA level.[24] The addition of low molecular-weight TEGDMA to decrease the viscosity contributes to a higher level of polymerization shrinkage than GD and Z3, which contain high molecular-weight monomers such as UDMA and Bis-EMA.

Many efforts to minimize polymerization stress by changing the resin composite formulation have been reported.[25-28] These efforts include the introduction of high-molecular-weight monomers (TCD-urethane or dimer dicarbamate dimethacrylate),[25] silorane-based resin composite,[26] and SDR (stress decreasing resin).[27,28] P9 is a silorane-based resin composite composed of a siloxane core and an oxirane ring. Its polymerization occurs via a cationic ring-opening reaction, resulting in a lower polymerization contraction compared with those of methacrylate-based resins, which polymerize via a radical addition reaction of their double bonds. The cationic cure starts with the generation of an acidic cation that opens the oxirane ring and generates a new acidic carbocation center. After the addition to an oxirane monomer, the epoxy ring is opened to form a chain or, in the case of two or multifunctional monomers, a network.[26] Volumetric expansion occurs during this process and compensates for the polymerization shrinkage. Because of the specific structure of P9, the manufacturer recommends using the P9 system adhesive self-etch primer.[29]

In this study, the XP bond was applied for evaluation in the same conditions as the other resin composites. It is not clear why there was relatively good internal adaptation, even though XP bond was used in P9. It might be connected with relatively lower polymerization shrinkage in P9 and poorer chemical reaction between XP bond and P9. Limited amounts of shrinkage stress would be experienced at the adhesive and the composite interface and this

would lead to better sealing by the underlying adhesive. Further study will be necessary.

Here, P9 has a lower polymerization shrinkage strain than the other five groups, and similar results have been previously reported.[30] In terms of the polymerization shrinkage stress, it has been reported that P9 does not show the lowest shrinkage stress.[31,32] It has also been reported that low-shrinkage resin composite materials may have less volumetric shrinkage but that their polymerization shrinkage stress is still similar to that of conventional resin composites.[33] This difference might be explained by the fact that the polymerization shrinkage stress was affected not only by volumetric shrinkage but also by the elastic modulus of the material, gel times, and so on. Resin composites that have the same volumetric shrinkage do not always generate the same stress. A resin composite with a higher elastic modulus generates higher polymerization shrinkage stress because the flow in the resin material is limited.[26] In the present study, however, P9 also showed the lowest polymerization shrinkage stress. This result might be explained by the low polymerization shrinkage strain compared with those of the methacrylate-based resin composites and the property, which delays the gel point.[34] P9 took the longest time to reach the gel point because of the time needed for cation formation; siloranes have a polymerization reaction with a slow onset. This means that the silorane resin composite possessed the highest potential for stress relief by permitting material flow during the initial curing stage.[34] As a result, P9 exhibited the lowest shrinkage stress, although P9 also showed a high elastic modulus of 9 GPa.

Comparing the results of polymerization shrinkage strain and stress, there was similarity in terms of material ranking. However, the order of Z3 and GD was changed. This discrepancy may be explained by differences in the elastic modulus of the resin composite and the polymerization shrinkage strain. For example, in the present study, the elastic modulus of Z3 was 11 GPa (Table 1) and its linear shrinkage was 10.4 μm, while the elastic modulus of GD was 6.3 GPa and its linear shrinkage was 13.40 μm. When the elastic modulus × linear shrinkage was calculated, which affects the polymerization shrinkage stress, this value was 114.4 GPa in Z3 and 84.42 GPa in GD. In the nonflowable resins Z3, GD, and CH, the composition of the resin composite affected its elastic modulus. The elastic moduli of the dimethacrylate polymers can be ranked as follows: TEGDMA < Bis-EMA < UDMA < Bis-GMA.[35] The UDMA-based resin composite GD exhibits lower polymerization shrinkage stress than the Bis-GMA–based resin composite Z3. It is not surprising that resin composites with higher polymerization shrinkage strain had higher polymerization shrinkage stress. However, the polymerization shrinkage stress is also affected by the composition of the resin composite and the elastic modulus, giving different results, according to previous findings.[36]

SD was reported to lower the polymerization rate and fill up to a 4-mm bulk filling.[27] Study on SD has shown that it has reduced volumetric shrinkage compared with conventional methacrylate-based flowable composites,[28] and it is consistent with the results of the present study. SD is composed of a urethane dimethacrylate structure that is responsible for the reduction in polymerization shrinkage and stress. This effect may be due in part to the larger size of the SD resin compared with TF (molecular weight of 849 g/mol for SD resin compared with 513 g/mol for Bis-GMA). The properties of SD are due to the combination of the large molecular structure with a chemical moiety called a "polymerization modulator" that is chemically embedded in the center of the polymerizable resin backbone of the SD monomer. The high molecular weight and the conformational flexibility around a centered modulator impart optimized flexibility, such that SD shows a lower polymerization shrinkage than methacrylate flowable resin.[37] In the limited results of the present study, SD showed superior internal adaptation to that of the conventional flowable resin TF, but it showed inferior internal adaptation compared with other nonflowable composites except CH. Further study will be necessary for clinical determination of its applicability.

In this study, the strain and stress rates were calculated at 10 seconds of light curing. The statistical results of polymerization shrinkage strain and stress were very similar to those of strain and stress rate (Tables 2 and 3). It means that early stress and strain rate are important factors to determine final shrinkage stress and strain.

The four null hypotheses in this study could be rejected because there were positive correlations between the %SP, the %RP, and polymerization shrinkage strain and stress (Table 6, $p<0.001$).

The proposed method, in which a silver nitrate solution was used to penetrate the pulp space through the dentinal tubules and the resulting amount of penetration into the microgap areas was assessed by micro-CT, may provide a new measure

for evaluating internal adaptation nondestructively. In addition, this method has the advantage that constant results were obtained reproducibly both before and after thermomechanical loading.

CONCLUSION

In this study, the polymerization shrinkage stress and strain were found to be closely related to the internal adaptation of the resin composite restorations. The newly proposed model for the evaluation of internal adaptation using micro-CT and silver nitrate may provide a new measurement for evaluating the internal adaptation of restorations in a nondestructive way.

Acknowledgement

This study was supported by the Basic Science Research Program through the National Research Foundation of Korea funded by the Ministry of Education, Science, and Technology (7-2009-0235).

Conflict of Interest

The authors of this manuscript certify that they have no proprietary, financial, or other personal interest of any nature or kind in any product, service, and/or company that is presented in this article.

(Accepted 24 May 2013)

REFERENCES

1. Bausch JR, de Lange K, Davidson CL, Peters A, & de Gee AJ (1982) Clinical significance of polymerization shrinkage of composite resins *Journal of Prosthetic Dentistry* **48(1)** 59-67.
2. Hashimoto M, Ohno H, Sano H, Kaga M, & Oguchi H (2003) *In vitro* degradation of resin-dentin bonds analyzed by microtensile bond test, scanning and transmission electron microscopy *Biomaterials* **24(21)** 3795-3803.
3. Souza-Junior EJ, de Souza-Regis MR, Alonso RC, de Freitas AP, Sinhoreti MA, & Cunha LG (2011) Effect of the curing method and composite volume on marginal and internal adaptation of composite restoratives *Operative Dentistry* **36(2)** 231-238.
4. Tay FR, & Pashley DH (2003) Water treeing—a potential mechanism for degradation of dentin adhesives *American Journal of Dentistry* **16(1)** 6-12.
5. Alani AH, & Toh CG (1997) Detection of microleakage around dental restorations: A review *Operative Dentistry* **22(4)** 173-185.
6. Kakaboura A, Rahiotis C, Watts D, Silikas N, & Eliades G (2007) 3D-marginal adaptation versus setting shrinkage in light-cured microhybrid resin composites *Dental Materials* **23(3)** 272-278.
7. Raskin A, Tassery H, D'Hoore W, Gonthier S, Vreven J, Degrange M, & Dejou J (2003) Influence of the number of sections on reliability of *in vitro* microleakage evaluations *American Journal of Dentistry* **16(3)** 207-210.
8. Zeiger DN, Sun J, Schumacher GE, & Lin-Gibson S (2009) Evaluation of dental composite shrinkage and leakage in extracted teeth using X-ray microcomputed tomography *Dental Materials* **25(10)** 1213-1220.
9. De Santis R, Mollica F, Prisco D, Rengo S, Ambrosio L, & Nicolais L (2005) A 3D analysis of mechanically stressed dentin-adhesive-composite interfaces using X-ray micro-CT *Biomaterials* **26(3)** 257-270.
10. Sun J, Eidelman N, & Lin-Gibson S (2009) 3D mapping of polymerization shrinkage using X-ray micro-computed tomography to predict microleakage *Dental Materials* **25(3)** 314-320.
11. Kwon OH, & Park SH (2012) Evaluation of internal adaptation of dental adhesive restorations using micro-CT *Journal of Korean Academy of Conservative Dentistry* **37(1)** 41-49.
12. Peutzfeldt A, & Asmussen E (2004) Determinants of *in vitro* gap formation of resin composites *Journal of Dentistry* **32(2)** 109-115.
13. Rosin M, Urban AD, Gartner C, Bernhardt O, Splieth C, & Meyer G (2002) Polymerization shrinkage-strain and microleakage in dentin-bordered cavities of chemically and light-cured restorative materials *Dental Materials* **18(7)** 521-528.
14. Gerdolle DA, Mortier E, & Droz D (2008) Microleakage and polymerization shrinkage of various polymer restorative materials *Journal of Dentistry for Children (Chicago, Ill)* **75(2)** 125-133.
15. Calheiros FC, Sadek FT, Braga RR, & Cardoso PE (2004) Polymerization contraction stress of low-shrinkage composites and its correlation with microleakage in class V restorations *Journal of Dentistry* **32(5)** 407-412.
16. Braga RR, Ferracane JL, & Condon JR (2002) Polymerization contraction stress in dual-cure cements and its effect on interfacial integrity of bonded inlays *Journal of Dentistry* **30(7-8)** 333-340.
17. Condon JR, & Ferracane JL (2000) Assessing the effect of composite formulation on polymerization stress *Journal of the American Dental Association* **131(4)** 497-503.
18. Chen X, Cuijpers V, Fan M, & Frencken JE (2009) Optimal use of silver nitrate and marginal leakage at the sealant-enamel interface using micro-CT *American Journal of Dentistry* **22(5)** 269-272.
19. Dietschi D, Olsburgh S, Krejci I, & Davidson C (2003) *In vitro* evaluation of marginal and internal adaptation after occlusal stressing of indirect class II composite restorations with different resinous bases *European Journal of Oral Sciences* **111(1)** 73-80.
20. Kinomoto Y, Torii M, Takeshige F, & Ebisu S (2000) Polymerization contraction stress of resin composite restorations in a model Class I cavity configuration using photoelastic analysis *Journal of Esthetic Dentistry* **12(6)** 309-319.
21. Oliveira LC, Duarte S Jr, Araujo CA, & Abrahao A (2010) Effect of low-elastic modulus liner and base as stress-absorbing layer in composite resin restorations *Dental Materials* **26(3)** e159-169.
22. Braga RR, Ballester RY, & Ferracane JL (2005) Factors involved in the development of polymerization shrinkage

stress in resin-composites: A systematic review *Dental Materials* **21(10)** 962-970.

23. Davidson CL, & Feilzer AJ (1997) Polymerization shrinkage and polymerization shrinkage stress in polymer-based restoratives *Journal of Dentistry* **25(6)** 435-440.
24. Charisma Scientific Information (2007). Retrieved online Mar, 05, 2013 from: http://heraeus-dental.com/media/webmedia_local/international/pdf/Charisma_ScientificInforation_GB_20080102.pdf
25. Braga RR, & Ferracane JL (2004) Alternatives in polymerization contraction stress management *Critical Reviews in Oral Biology and Medicine* **15(3)** 176-184.
26. Weinmann W, Thalacker C, & Guggenberger R (2005) Siloranes in dental composites *Dental Materials* **21(1)** 68-74.
27. Roggendorf MJ, Kramer N, Appelt A, Naumann M, & Frankenberger R (2011) Marginal quality of flowable 4-mm base vs. conventionally layered resin composite *Journal of Dentistry* **39(10)** 643-647.
28. Ilie N, & Hickel R (2011) Investigations on a methacrylate-based flowable composite based on the SDR technology *Dental Materials* **27(4)** 348-355.
29. Filtek P90 Scientific Information (2007) *3M ESPE*.
30. Ilie N, Jelen E, Clementino-Luedemann T, & Hickel R (2007) Low-shrinkage composite for dental application *Dental Materials Journal* **26(2)** 149-155.
31. Marchesi G, Breschi L, Antoniolli F, Di Lenarda R, Ferracane J, & Cadenaro M (2010) Contraction stress of low-shrinkage composite materials assessed with different testing systems *Dental Materials* **26(10)** 947-953.
32. Boaro LC, Goncalves F, Guimaraes TC, Ferracane JL, Versluis A, & Braga RR (2010) Polymerization stress, shrinkage and elastic modulus of current low-shrinkage restorative composites *Dental Materials* **26(12)** 1144-1150.
33. Tantbirojn D, Pfeifer CS, Braga RR, & Versluis A (2011) Do low-shrink composites reduce polymerization shrinkage effects? *Journal of Dental Research* **90(5)** 596-601.
34. Gao BT, Lin H, Zheng G, Xu YX, & Yang JL (2012) Comparison between a silorane-based composite and methacrylate-based composites: Shrinkage characteristics, thermal properties, gel point and vitrification point *Dental Materials* Journal **31(1)** 76-85.
35. Sideridou I, Tserki V, & Papanastasiou G (2003) Study of water sorption, solubility and modulus of elasticity of light-cured dimethacrylate-based dental resins *Biomaterials* **24(4)** 655-665.
36. Park S LS, Cho Y, & Kim S (2003) Amount of polymerization shrinkage and shrinkage stress in composites and compomers for posterior restoration *Journal of Korean Academy of Conservative Dentistry* **28(4)** 348-353.
37. Scientific Compendium SDR (2011) *Dentsply*.